www.ptcer.pl/mccm

MATERIAŁY CERAMICZNE /CERAMIC MATERIALS/, 64, 2, (2012), 156-161

Transport Phenomena and Diffusion Anomalies in Glass

Helmut A. Schaeffer*

e-mail: helmut.schaeffer@gmx.net

Abstract

Mass transport processes in glass can be differentiated according to the type of diffusion species: gases, network modifiers and network formers. The mobilities of these species give rise to a variety of diffusion-controlled processes and properties. Interface reactions (such as dissolution of sand grains by sodium silicate melts, corrosive attack of refractory material by glass melts, devitrification in a soda-lime-silica glass) will be discussed where the chemical potential is the driving force for establishing „up-hill" diffusion profiles. With the help of phase diagrams the diffusion pathways can be predicted. The formation of the tin concentration maximum ("tin hump"), which is found in near-surface regions at the bottom side of float glass, is a further example of up-hill diffusion, in this case induced by redox reaction. The result of the mixed-alkali effect of a homogenously melted soda-potassia-lime-silica glass series and of an ion-exchanged glass (soda-lime-silica glass treated in KNO_3) is compared with respect to their electrical resistivity. In ion-exchanged glass only sodium acts as a charge carrier, whereas in regular mixed-alkali glasses both alkalis can be responsible for electrical conduction. Moreover, sodium diffusion anomalies in SiO_2 glasses are reviewed and a possible mixed-alkali effect on the impurity level between sodium and the OH content is revealed. A further sodium diffusion anomaly (sharp increase of mobility) was detected in silica glass at the temperature of the α-β quartz phase transformation, thus indicating that a preordered quartz-type structure seems to exist in silica glass. Finally, the role of the diffusivities of network oxygen, molecular oxygen and silicon in silica glass is interpreted. The oxygen mobilities govern the growth of passivating SiO_2 layers on silicon-containing materials (such as silicon, silicon carbide, silicon nitride) whereas the silicon mobility is responsible for viscous flow.

Keywords: Ionic diffusivity, Mixed-alkali effect, Diffusion anomaly, Interface reaction, Diffusion-controlled process

ZJAWISKA TRANSPORTOWE I ANOMALIE DYFUZJI W SZKŁACH

Procesy transportu masy w szkle mogą być zróżnicowane w zależności od typu dyfundujących składników: gazy, modyfikatory sieciowe i składniki więźbotwórcze. Ruchliwości tych składników dają przyczynek do powstania rozmaitości procesów kontrolowanych dyfuzją i właściwości. Omówione zostaną reakcje takie jak rozpuszczanie cząstek piasku przez stopy sodowo-krzemianowe, korozyjny atak stopów szklanych na materiały ogniotrwałe, dewitryfikacja w szkle sodowo-wapniowo-krzemionkowym, zachodzące na powierzchni rozdziału faz, w których potencjał chemiczny jest siłą napędową ustalania się profili dyfuzji wstępującej. Tworzenie się maksimum stężenia cyny („garb cynowy"), które znajdowane jest w obszarach przypowierzchniowych na stronie dolnej szkła płaskiego z metody *float*, jest następnym przykładem dyfuzji wstępującej, w tym przypadku wywołanej przez reakcje *redox*. Porównuje się wpływ efektu mieszanego alkalicznego w przypadku jednorodnie stopionej serii szkła sodowo-potasowo-wapniowo-krzemionkowe i wymiany jonowej w szkle (szkło sodowo-wapniowo-krzemionkowe) na rezystywność elektryczną szkieł. W szkle pochodzącym z wymiany jonowej jedynie sód działa jako nośnik ładunku elektrycznego, podczas gdy w normalnych szkłach otrzymanych z mieszaniny alkaliów obydwa składniki alkaliczne mogą być odpowiedzialne za przewodnictwo elektryczne. Ponadto, przeglądowi poddane są anomalie dyfuzji sodu w SiO_2, aby ujawnić możliwy wpływ efektu mieszanego alkalicznego na poziom zanieczyszczeń pomiędzy zawartością sodu i OH. Na koniec, interpretacji poddawana jest rola dyfuzyjności tlenu sieciowego, tlenu cząsteczkowego i krzemu w szkle krzemionkowym. Ruchliwość tlenu rządzi wzrostem pasywujących warstw SiO_2 na materiałach zawierających krzem takich jak krzem, węglik krzemu i azotek krzemu, podczas gdy ruchliwość krzemu odpowiedzialna jest za płynięcie lepkościowe.

Słowa kluczowe: dyfuzja jonowa, mieszany efekt alkaliczny, anomalia dyfuzji, reakcja na granicy miedzyfazowej, proces kontrolowany dyfuzją

1. Introduction – Driving forces for transport phenomena

The two common diffusion equations, 1st (Eq. 1) and 2nd (Eq. 2) Fick's Law characterize mass transport insufficiently. The equations describe diffusion processes only in a concentration gradient ($\partial c/\partial x$).

$$j = D\,(\partial c/\partial x) \quad (1)$$

$$\partial c/\partial t = D\,(\partial^2 c/\partial x^2) \quad (2)$$

The more general formulation requires the substitution of the concentration gradient by the gradient of the chemical potential ($\partial \mu/\partial x$), i.e. the gradient of Gibbs free enthalpy. This

*Professor Emeritus of Materials Science, University of Erlangen-Nûrnberg, Retired Director- Deutsche Glastechnische Gesellschaft and the Research Association of the German Glass Industry, Past President- International Commission on Glass (2000-2003).

gradient is the overall driving force and often mass transport does not follow the gradient of concentration of a particular species. Thus, thermodynamics overrules kinetics or more precisely thermodynamics determines the kinetic behaviour of a multi-component system.

In the following, examples for transport phenomena in glass will be given which appear as diffusion anomalies when viewing them as driven by concentration gradients, but are quite normal when evaluated thermodynamically. These transport phenomena are coined as „up-hill" diffusion, since mass transport proceeds opposite to the concentration gradient. The simplest case of up-hill diffusion is observed when a particular species which has different solubilities in two different liquids is enriched or depleted in the respective liquids, i.e. the enrichment follows the gradient of chemical potential thereby extracting the species in question against its concentration gradient.

Phase diagrams are a helpful tool to understand and predict what happens when two differently composed systems are in contact and start to interact which each other. These diagrams reflect the thermodynamic equilibrium of a system. The melting points of particular compounds in the phase diagram indicate regions of thermodynamic stability. The higher the melting point the more stable the compound; therefore, the chemical potential exerts kinetically a driving force on the existing components to realize the compound formation.

2. Transport phenomena explained by phase diagrams

2.1. Na_2O-SiO_2 – system: Dissolution of silica by sodium silicate

In this phase diagram the sodium metasilicate ($Na_2O{\cdot}SiO_2$) displays the highest melting point (higher than for the orthosilicate and the disilicate) and therefore is thermodynamically the most stable compound, see Fig. 1.

As a result when quartz grains or silica react with sodium oxide or sodium silicate melts, an enrichment of sodium takes place at the reaction interface. This enrichment is driven thermodynamically since the system tends to establish an equilibrium by forming the sodium metasilicate. It was observed that sodium oxide is enriched by up to 25 wt% at a quartz grain surface in a soda-lime-silica glass melt containing 13.5 wt% sodium oxide [1]. The effect was even more pronounced when fused silica reacted with a sodium silicate melt (8 wt% Na_2O); here the sodium oxide enriched up to 40% at the reaction interface, see Fig. 2.

The order of the flux efficiency of alkali oxides in glass melting is reflected by the increasing melting point of alkali silicates with higher amounts of alkali: ($K_2O{\cdot}2SiO_2$: 1045°C; $Na_2O{\cdot}SiO_2$: 1090°C; $2Li_2O{\cdot}SiO_2$: 1255°C).

2.2. Na_2O-Al_2O_3-SiO_2 – system: Corrosion of refractory material

This phase diagram serves as a model diagram for the reaction of glass melts with refractory material (see Fig. 3). The glass composition and the composition of a refractory brick (e.g. 20 wt% Al_2O_3, 80 wt% SiO_2) are marked in Fig. 3.

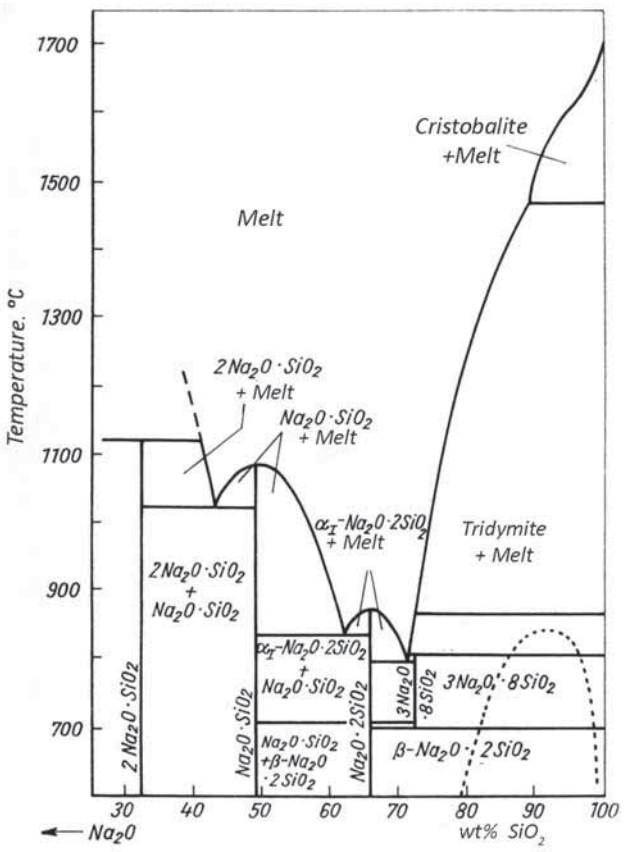

Fig. 1. Phase diagram Na_2O–SiO_2.

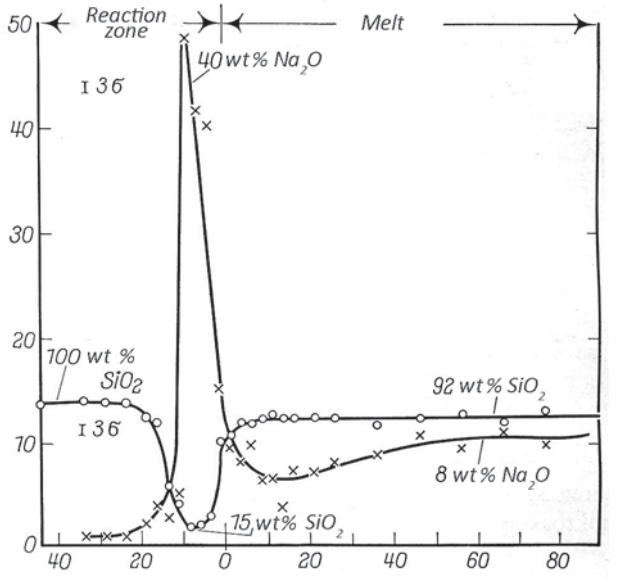

Fig. 2. Up-hill diffusion of sodium at the interface SiO_2 glass/ sodium silicate melt [2].

At melting temperatures one would expect a corrosion reaction (diffusion path) along the dashed line. However, the reaction path takes a detour since nepheline, the compound with the highest melting point, enforces the deviation along the solid line in Fig. 3. It is observed that refractories in glass tanks show nepheline formation as a corrosion product after long service life.

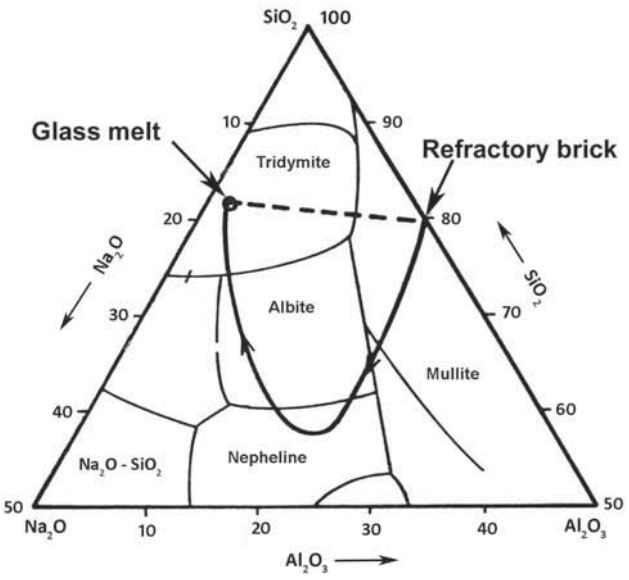

Fig. 3. Reaction path (solid line) between refractory brick and glass melt [3].

Typical soda-lime-silica glass melts contain about 13 wt% Na_2O, thus an up-hill diffusion takes place to form nepheline with about 22 wt% Na_2O.

2.3. Na_2O-CaO-SiO_2 – system: Devitrification

Crystallisation from a glass melt matrix, so-called devitrification, involves per se a rearrangement of elements which leads to local compositional enrichments and depletions. The formation of devitrite from a soda-lime-silica glass melt (16 Na_2O, 10 CaO, 74 SiO_2 in wt%) is a typical example of up-hill diffusion as shown in Fig. 4. The crystallization of devitrite containing 10.5 wt% Na_2O and 275 wt.% CaO requires a calcium enrichment and a sodium depletion. In the case shown in Fig. 4 the crystallization is not completed yet. The concentration profiles reveal the necessary preordering of species prior to final crystallization.

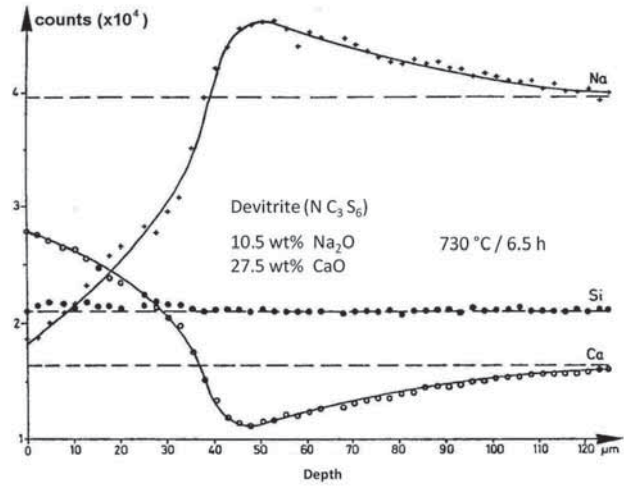

Fig. 4. Up-hill diffusion due to surface devitrification of a soda-lime-silica glass [4].

3. Complex up-hill diffusion: The „tin hump" in float glass

Float glass which is in contact with molten tin in the float chamber during its forming process shows a tin uptake which starts as an error-function type diffusion profile, but then at depths of about 10 µm the tin concentration increases and displays a „hump", see Fig. 5. The thicker the float glass, i.e. the longer the contact of the glass with the tin bath the more pronounced the tin peak. For the understanding of this phenomenon it is important to know that highly reduced melted float glass (under reduced pressure, „vacuum refining") lacks the tin hump. Therefore, this particular up-hill diffusion is related to redox interactions. The assumed redox reactions and diffusion processes are listed in Table 1. The divalent Sn^{2+} diffuses into the bottom side of the float glass, the deeper it proceeds the more Fe^{3+} is present (the near-surface region is depleted of iron) and Sn^{2+} is oxidized to Sn^{4+} whereas iron is reduced to Fe^{2+}. The Sn^{4+} is less mobile than the Sn^{2+} therefore the tin is immobilized and piles up forming the hump [7]. The reduced melted glass contains basically no trivalent iron, therefore the transformation to Sn^{4+} does not occur and the tin (Sn^{2+}) profile can extend smoothly into the glass.

Table 1. Chemical reactions in float chamber [6, 7].

Tin / Glass:

$Sn^0 + Na_2O$ (glass) $\rightarrow 2Na^0 + SnO$ (glass)
$Sn^0 + FeO$ (glass) $\rightarrow Fe^0 + SnO$ (glass)

Glass:

Sn^{2+}(surface)+Ca^{2+}(structure)$\rightarrow Sn^{2+}$(structure)+Ca^{2+}(surface)
$Sn^{2+} + Fe^{3+} \rightarrow Sn^{4+} + Fe^{2+}$

Chamber Atmosphere:

$Sn^0 + ½\ O_2 \rightarrow SnO\ \uparrow$
$Sn^0 + S$(glass) $\rightarrow SnS\ \uparrow$
$SnS + H_2 \rightarrow Sn + H_2S$

Tin / Bottom Refractory

$2Na^0 + ½\ O_2 \rightarrow Na_2O$
$Na_2O + Al_2O_3/SiO_2 \rightarrow Na[Al\ SiO_4]$ (nepheline)

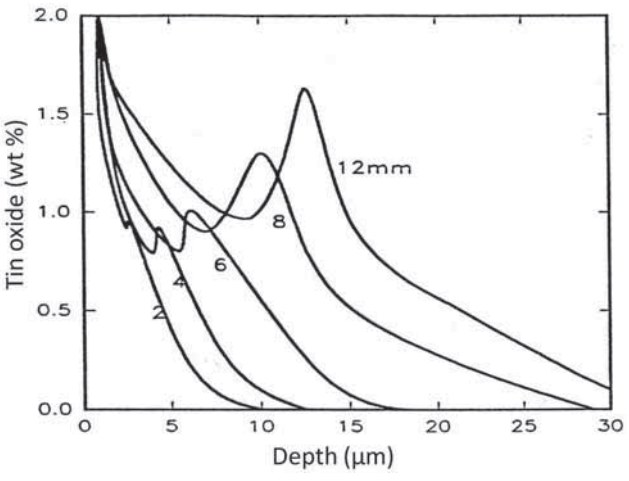

Fig. 5. Tin concentration profiles with „hump" of float glass (bottom side) [5].

4. The mixed-alkali effect

Few transport phenomena in glass science have been debated with such an endurance and with such a diversity of approaches as is the case with the mixed-alkali effect. The effect consists of the following: Adding a second type of alkali ion into a single alkali silicate glass changes a variety of properties in a non-linear fashion. The properties which are most affected are those based on the diffusivities of the alkali species, e.g. self-diffusion, electrical conductivity, internal friction.

The mixed-alkali effect is impressively reflected in the electrical conductivity which is related to the alkali ions as

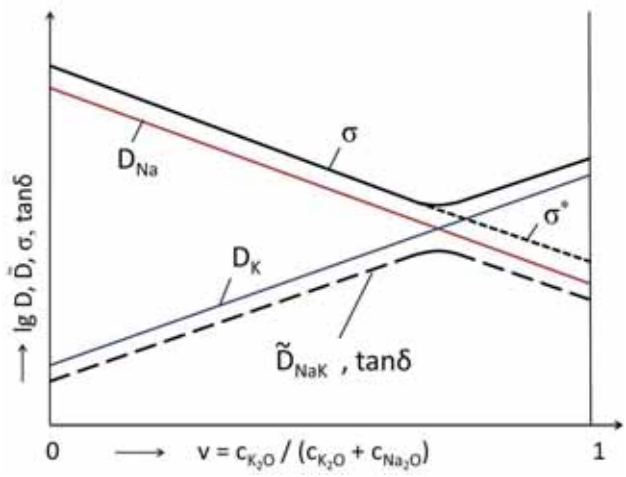

Fig. 6. Scheme of the mixed-alkali effect of a soda-potassia-silica glass;
D_{Na}, D_K – self-diffusion coefficients,
D_{NaK} – interdiffusion coefficient,
σ – electrical conductivity,
σ^* – electrical conductivity of ion-exchanged glass,
tanδ – loss angle (internal friction),
v – mole fraction.

charge carriers. In a good approximation the Nernst-Einstein equation holds, i.e. the conductivity can be expressed by the self-diffusion coefficients of the two involved alkali ions (e.g. potassium and sodium) as a function of their molar ratio, $v = c_{K_2O}/(c_{K_2O} + c_{Na_2O})$.

Fig. 6 shows schematically the concentration dependence of the self-diffusion coefficients and the resulting electrical conductivity. Depending on the molar ratio the most mobile alkali ion is responsible for the electrical transport. In the sodium rich glass ($v << 0.7$) it is the Na^+ ion, in the potassium rich glass ($v >> 0.7$) it is the K^+ ion. In the vicinity of $v \approx 0.7$ the minimum of diffusivities can be found and thus the minimum of electrical conductivity (or the maximum of electrical resistivity) at levels which are orders of magnitude different from those of the corresponding single alkali glasses.

Fig. 6 further shows that certain transport phenomena depend on the least mobile alkali ions. This is displayed by the dashed line. For instance, internal friction (mechanical loss) is governed by the least mobile alkali ions and so is the interdiffusion coefficient which controls ion exchange processes. Therefore, the dashed line stands either for the loss angle or the interdiffusion coefficient.

As an example in Fig. 7 the electrical resistivity of a soda-lime-magnesia mixed alkali glass (total alkali content 10 mol.%) is shown. The maximum of the resistivity is observed at $v \approx 0.7$ (200 °C).

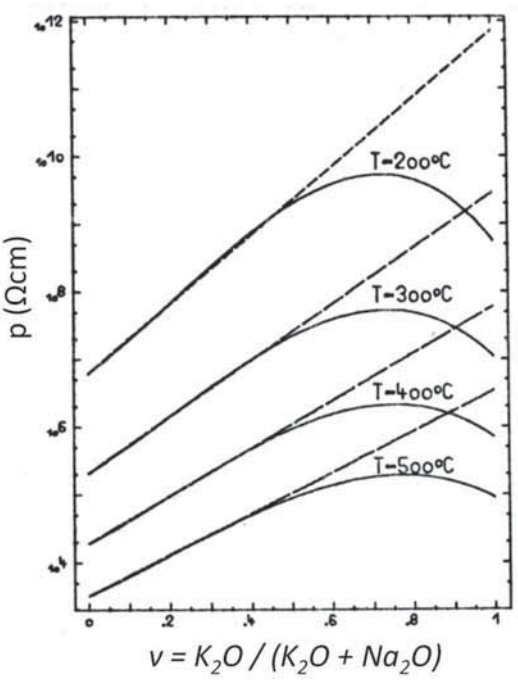

Fig. 7. Electrical resistivity versus mole fraction for homogeneously melted mixed-alkali glasses (solid lines) and ion-exchanged glass (dashed lines) [8].

Furthermore, the resistivity of an ion-exchanged glass (dotted line) is plotted in Fig. 7. A sodium containing glass was ion-exchanged in a potassium nitrate melt. In this way a mixed-alkali glass series is formed in a near-surface region. Instead of maxima in the resistivity curves now straight lines occur with the maximum resistivity at the surface ($v = 1$) of the ion-exchanged glass [8]. Over the whole range of composition only sodium ions are the electrical charge carriers and ion-exchanged glasses possess a steep gradient of electrical resistivity between the surface and the interior (up to six orders of magnitude).

The difference is attributed to the fact that the ion exchange below T_g causes a different glass structure as the melting of mixed-alkali glasses. It could be shown that the resulting compressive stresses exerted by the larger potassium ion are not responsible, even though the difference to the homogeneously melted mixed-alkali glasses vanishes when heat-treating ion-exchanged glasses above T_g.

The real cause of the non-linearity of the mixed-alkali effect is still not fully understood. However, a pathway model for alkali mobility is predominantly accepted [9, 10]. This model assumes that alkali ions migrate along type-specific pathways or channels (of a certain length distribution). The proximity and/or crossing of different pathways apparently blocks the transport of ions rather effectively since a blocked pathway hinders the transport of numerous ions („traffic jam" effect explains non-linearity) [10].

On the other hand, the ion exchange cannot establish the type-specific pathway for potassium below T_g and therefore the mixed-alkali effect does not occur, but can be restored after structural rearrangement above T_g.

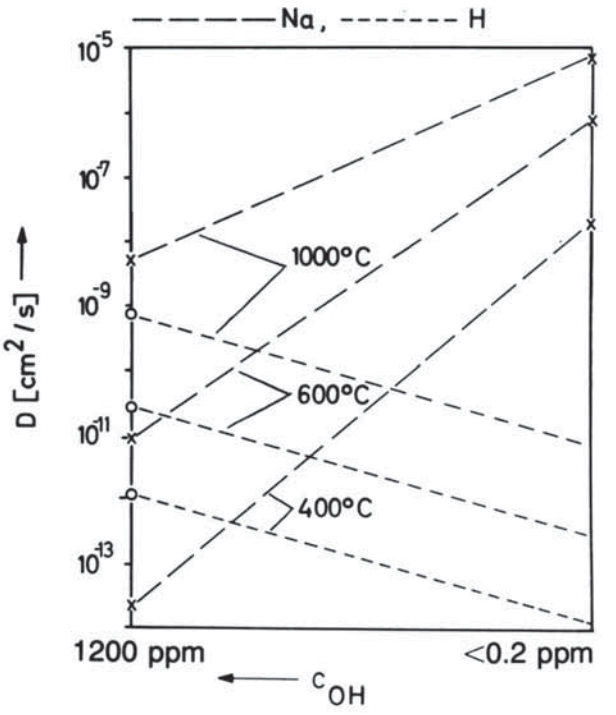

Fig. 8. Ionic diffusivities of sodium and hydrogen as a function of OH content in silica glasses (schematic diagram of mixed-alkali effect) [11].

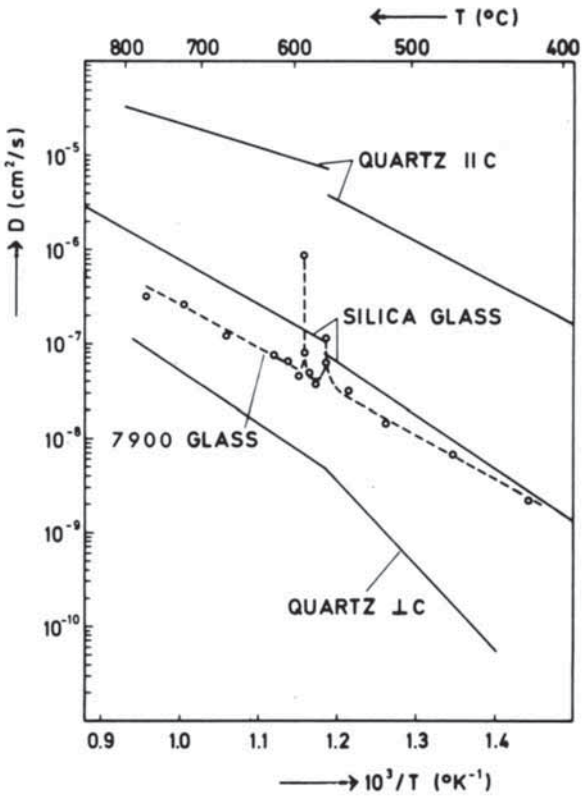

Fig. 9. Sodium diffusivities and diffusion anomalies in quartz, silica glass and Vycor® glass [12-14].

5. Diffusion anomalies in silica glass

5.1. Mobility of trace elements

Using ^{23}Na and ^{3}H (tritium) as radiotracers, mobilities of sodium and hydrogen ions in various types of SiO_2 glasses of different OH content have been studied. It was found that the diffusion coefficients depend on the OH content in the silica network. Increasing OH content considerable reduces the Na diffusivities, but increases the hydrogen mobilities. The effect of mutual immobilization shows similarities with the mixed-alkali effect and follows the reasoning in the literature that the hydrogen ion behaves like an alkali ion in transport phenomena, see Fig. 8.

The higher immobilization of sodium ion impurities with increasing OH content in silica is relevant when utilizing thin SiO_2 layers as passivating barriers for ionic transport. Their blocking power is more pronounced with higher OH content.

5.2. Sodium diffusion peaks („Hedvall effect")

Tracer diffusion data achieved with ^{23}Na in quartz as well as silica glass and Vycor® glass (96% SiO_2) show discontinuities or even diffusion peaks at particular temperatures, see Fig. 9. At about 570 °C the quartz as well as the glass samples display an abrupt change in the sodium diffusion; in the Vycor glass even a further diffusion peak is observed. It appears obvious to relate the anomalies with the α-β-quartz transformation (573 °C) which may occur in the glass structure due to preordered regions which resemble the quartz modification. The ongoing structural rearrangement is reflected in an increased sodium mobility. Such effects have been observed previously by J.A. Hedvall in crystalline silicates at temperatures of phase transformations and have been explained by the reorientation of the crystal lattice imparting high mobilities of all species and thus causing maxima of reactivity („Hedvall effect").

In the Vycor glass the sodium diffusivity not only peaks at 570 °C, but also at 590 °C [14]. The nature of the structural rearrangement at 590 °C is unsolved. It might be speculated that the enhanced diffusion is related to the previous fabrication procedure (phase separation, leaching and sintering process) which the Vycor glass has undergone.

6. Diffusion-controlled processes in silica glass

As an example, fused silica glass is chosen to demonstrate how the mobilities of atomic species are correlated with the macroscopic properties.

Fig. 10 shows the wide range of diffusion coefficients of various species in SiO_2 glass which spans over 16 orders of magnitude – from helium as the fastest to silicon as the slowest species [15].

The diffusion data also provides a qualitative insight into the glass structure. Helium and hydrogen are gases with extremely high diffusivities indicating the open network of the SiO_2 glass structure. They diffuse much slower in soda-lime-silica glasses where the network-modifying cations partially block the pathways for gas permeation. The diffusivities of gases depend on the diameter of the gas molecules, i.e. following helium and hydrogen they decrease in the order oxygen, argon and nitrogen. Water vapor diffuses via an interaction with the silica network by forming Si-OH groups. Sodium is the fastest of the incorporated

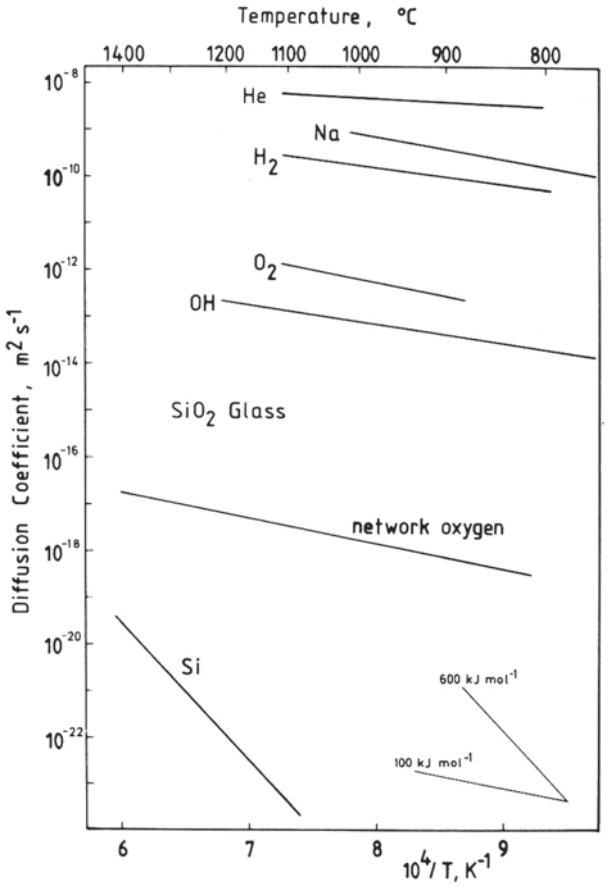

Fig. 10. Diffusivities of gases, network modifiers and network formers in silica glass as a function of temperature [15].

species (Si-O-Na), whereas network oxygen (Si-O-Si) and silicon are by far the slowest.

The network oxygen diffusion is correlated with the O_2 diffusion and plays an important role in the oxidation process of silicon, but also of silicon carbide and silicon nitride, in forming SiO_2 glass layers. The growth of these layers is governed by a parabolic rate constant which is directly related to the diffusion of network oxygen and molecular oxygen. Therefore, all three phenomena possess the same activation energy [16].

Finally, the diffusion of silicon (D_{Si}) [17] is correlated with the viscosity η (both have identical activation energies). Surprisingly the Stokes-Einstein equation (Eq.(3), derived only for macroscopic systems) predicts flow units in the order of atomic dimensions (d ≈ 0.3 nm), triggering suggestions that viscosity is determined by the mobility of the silicon atoms or SiO_4 units [16].

$$D_{si} \cdot \eta / k \cdot T = 1/2\pi \cdot d \qquad (3)$$

Moreover, silicon diffusion appears to be rate-determining for high-temperature creep in silicon carbide and silicon nitride with their silica-rich grain boundaries. Inserting D_{Si} into the Coble creep formula results in creep rates which closely correspond to the experimental data [18].

7. Summary

The mobilities of network formers, modifiers and gases as well as the thermodynamic boundary conditions (reflected in the phase diagrams) are the basis to understand transport processes in glasses, such as up-hill diffusion, interface reactions, crystallization, mixed-alkali effect, ion exchange and diffusion-controlled phenomena.

8. References

[1] Löffler J.: „Diffusion processes around a sand grain", Glastech. Ber., 30, (1957), 129-133.

[2] Röttenbacher R., Mörtel H., Schaeffer H.A.: „Reaction processes between SiO_2 and a sodium silicate melt, Part 2. Reactions at the phase boundary", Glastech. Ber., 49, (1976), 278-284.

[3] Dietzel A.: „Correlation between phase diagrams, reaction paths and structure of melts", Glastech. Ber., 40, (1967), 378-381.

[4] Schaeffer H.A.: „Modifications and value-added processes of glass surfaces", in Werkstoff Glas II (Lohmeyer S. Ed.), Expert Verlag, Ehningen (1987), 1-25.

[5] Sieger J.S.: „Chemical characteristics of float glass surfaces", J. Non-Cryst. Solids, 19, (1975), 213-220.

[6] Franz H.: „Ion exchange and redox reactions in the float bath", Glastech. Ber. Glass Sci. Technol., 68 C 1, (1995), 15-20.

[7] Heide G., Müller-Fildebrandt C., Moseler D., Frischat G.H., Meisel W., Maldener A., Zouine-Thimm A., Rauch F.: „Tin in float glass: A diffusion-reaction model based on surface analysis explains the tin hump", Glastech. Ber. Glass Sci. Technol., 73, C 2, (2000), 321-330.

[8] Tomandl G., Schaeffer H.A.: „Relation between the mixed-alkali effect and the electrical conductivity of ion-exchanged glasses", Non-Crystalline Solids, Trans.Tech.Public. (1977), 480-485.

[9] Varshneya A.K.: „Data on ionic diffusion and electrical conduction in glass", in Fundamentals of Inorganic Glasses (Varshneya A.K. Ed.), Society of Glass Technology, Sheffield (2006), 2nd ed., 390-397.

[10] Tomandl G., Schaeffer, H.A.: „The mixed-alkali effect – A permanent challenge", J. Non-Cryst. Solids, 73, (1985), 179-196.

[11] Schaeffer H.A., Mecha J., Steinmann J.: „Mobility of sodium ions in silica glass of different OH content", J. Am.,Ceram.,Soc., 62, (1979), 343-346.

[12] Frischat G.H.: „Sodium diffusion in natural quartz crystals", J. Am. Ceram. Soc., 53, (1970), 357.

[13] Frischat G.H.: „Anomalous diffusion behavior of sodium in SiO_2 glass: I", Phys. Chem. Glasses, 11, (1970), 25-29.

[14] Schaeffer H.A. and Mecha, J.: „Sodium diffusion anomaly in high-silica glass", J. Am. Ceram. Soc., 57, (1974), 535.

[15] Schaeffer H.A.: „Diffusion-controlled processes in glass-forming melts",J. Non-Cryst. Solids 67, (1984), 19-33.

[16] Schaeffer H.A.: „Oxygen and silicon diffusion-controlled processes in vitreous silica", J. Non-Cryst. Solids, 38/39 (1980), 545-550.

[17] Brebec, G., Seguin, R., Sella, C., Bevenot J., Martin J.C.: „Diffusion of silicon in amorphous silica", Acta Metallurgica, 28, (1980), 327-333.

[18] Schaeffer H.A.: „Structure-property relationships of the vitreous state", in Progress in Nitrogen Ceramics (Riley F.L., Ed.), Martinus Nijhoff Publishers, Boston, The Hague, Dordrecht,Lancaster, (1983), 303-321.

♦

Received 20 July 2012; accepted 30 July 2012